

Modelling and Control of an Elastically Joint-Actuated Cart-Pole Underactuated System

Pengcheng Liu¹ (PhD student), Hongnian Yu¹ and Shuang Cang²

¹ Faculty of Science and Technology, Bournemouth University, Poole, UK

² School of Tourism, Bournemouth University, Poole, UK

Abstract—This paper investigates the modelling and closed-loop tracking control issues of a novel elastic underactuated multibody system. A torsional inverted pendulum cart-pole system with a single rotary actuator at the pivot of the cart is proposed. The system dynamics which incorporates with motion planning is firstly described. An optimization procedure is then discussed to plan the feasible trajectories that not just meet the performance requirements but also obtain optimality with respect to the cart displacement and average velocity. A closed-loop tracking controller is designed under collocated partial feedback linearization (CPFL). Subsequent presentation of simulation demonstrates that the proposed system is promising as compared to the previous work. The paper concludes with the application of our novel scheme to the design and control of autonomous robot systems.

Keywords- inverted pendulum; elasticity; underactuated dynamic system; tracking control

I. INTRODUCTION

Long term practical utility of inverted pendulum systems as benchmark for new control techniques has demonstrated the useful effect of various control approaches in such a manner that approximate the control issue of systems in real circumstances, as well as standard laboratory exercise for students at a number of universities and colleges. Moreover, the interest in studying the dynamics of the inverted pendulum arises from the fact that they are very similar to the dynamics that can be found in the systems need to be stabilized like rockets, missiles, ships, satellites, legged robots, marine tower, capsule robots, ropeway carriers, elastic joint robots, underwater vehicles.

Unlike dealing with the problem of upward pendulum stabilization which stabilize the system around its unstable equilibrium point, a trajectory tracking issue was raised and investigated in our previous works [1-6], which replace the force on the cart by a control input torque applied on the pivot to rotate the pendulum. As an underactuated mechanical system, one of the distinguished features of this system is that the friction dominates the whole system which is elliptically simplified or omitted in other underactuated mechanical systems. Numerous challenge issues concerning the control, optimization and trajectory planning have been identified and studied. The work [3] developed a closed-loop tracking control law with a six-step motion strategy were studied. Optimization and an open-loop control law were studied by Liu et al. [1]. A switch control method, in turn, which is robust against uncertainties and simply to implement, was

introduced in [2]. With the comparison to the closed-loop control law, a novel fuzzy control method was investigated in [4]. Based on the dynamic model, Liu et al. proposed an open-loop control law, a closed-loop control law, and a simple switch control law in [5]. Optimization and closed-loop control method was studied in [6] for the trajectory planning of the system.

This paper investigates an elastically joint-actuated cart-pole underactuated system based on our previous work [3]. The torque actuator articulated with a torsional spring designed in this paper is one of the distinguished features of the proposed system. Many animals are able to reduce the metabolic cost of running considerably by utilizing the elastic properties of muscles, tendons, and bones distributed in their bodies [7] and limbs [8]–[11]. In fact, springs for energy storage are pervasive in nature, and three generic uses of springs in biological systems are discussed by Alexander [12].

The majority of elastic actuator mechanisms are based on the series elastic actuator (SEA) configuration [13]. Elastic actuator has the advantage of high bandwidth mechanical compliance and can be used in force control. To increase suitability for different situations, a number of mechanisms extend the SEA allowing what is termed variable, adjustable or controllable stiffness. Adding compliance reduces the bandwidth and requires more control effort. Different groups ([14], [15]) examined the behavior and the controllability of elastic actuator and came to the conclusion that this actuation method is ideal for a lot of applications, for example haptic devices, legged robots or medical rehabilitation devices. This is widely existed where low impedance and high shock tolerance are more important than a high bandwidth [16] - [19]. There are two different ways of saving energy for mobile robots by using springs [20]. For losses of kinetic and potential energy, springs might be used to store and release a certain amount of the wasted energy. Another chance of reducing power consumption is when the link swings with a certain velocity, then at each end of the forward and backward swinging, the energy could be stored and released in springs.

The rest of the paper is organized as follows. In section II, the motion generation principle and dynamic model are developed. Section III and section IV investigate system constraints and the optimization procedure to achieve parametric selection. A closed-loop tracking controller is developed in section V. Numerical simulations of the proposed system are presented in section VI. Finally, conclusions are given in section VII.

II. SYSTEM DYNAMICS

A. Description of the system

The elastically joint-actuated cart-pole system used in this paper is shown in Fig.1. This simple multibody system consists of a cart and an inverted pendulum. The pendulum is mounted on the top of the cart which is in contact with a sufficiently wide horizontal ground surface through four passive wheels. A torque motor articulated with a torsional spring is put on the pendulum pivot to swing the pendulum instead of applying the force on the cart.

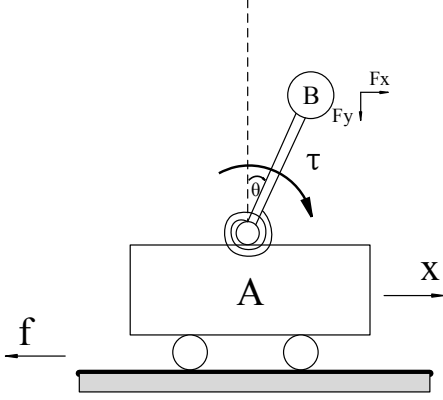


Figure 1. Elastically joint-actuated cart-pole system

The torque of motor actuation affects the angle of the pendulum from vertical by force couples as well as the displacement of the cart in the horizontal direction. Therefore, both of the angular velocity of the inverted pendulum and the displacement of the cart can be controlled through only one actuator. Table 1 summarizes the parameters of the proposed system.

B. Definitions and assumptions

In this paper, assumptions are made that the pendulum rod has neither mass nor inertia, and the center of mass of the whole inverted pendulum is coincide with the center of the ball which is fixed rigidly at the end of the pendulum. Furthermore, the air frictional resistance is supposed to be zero when the pendulum is rotating. The torsional spring is un-stretched when the inverted pendulum is upright.

TABLE I. PARAMETERS OF THE PROPOSED SYSTEM

Symbol	Description
A	rigid body I - the cart
B	rigid body II - the inverted pendulum
M (Kg)	mass of cart
m (Kg)	mass of ball
l (m)	length of inverted pendulum
θ (rad)	pendulum angle from vertical
k (N*m*rad ⁻¹)	elastic coefficient of the torsional spring
c (Kg*m ² *s ⁻¹ *rad ⁻¹)	coefficient of the viscous damper
g (m*s ⁻²)	gravitational acceleration
μ (N*m ⁻¹ *s ⁻¹)	coefficient of the friction between cart and ground
τ (N*m)	torque generated by the motor
F_x (N)	force applied on the ball in the horizontal direction
F_y (N)	force applied on the ball in the vertical direction
f_{max} (N)	the maximal static friction of the cart
Γ_i	position of point where force is applied
Q_i	generalized forces
P_1 (rad*s ⁻¹)	desired maximum joint velocity

Symbol	Description
P_2 (rad*s ⁻¹)	desired minimum joint velocity
P_3 (rad*s ⁻¹)	desired joint velocity at reflection point when the cart begins to keep still
ξ (rad*s ⁻²)	the critical value of the pendulum acceleration when the cart keeps still
$\Upsilon_i(\dot{q})$	Rayleigh dissipation function

C. Equations of motion

Let the generalized coordinates be:

$$[q_1, q_2]^T = [x, \theta]^T \quad (1)$$

The equations of motion of the proposed system can be achieved as a matrix form

$$\begin{cases} M_{11}(q_1)\ddot{q}_1 + M_{12}(q_1)\ddot{q}_2 + N(q_1, \dot{q}_1, q_2, \dot{q}_2) = Q_1 \\ M_{21}(q_1)\ddot{q}_1 + M_{22}(q_1)\ddot{q}_2 + N(q_1, \dot{q}_1, q_2, \dot{q}_2) = Q_2 \end{cases} \quad (2)$$

where $Q = [0, \tau]^T$ is the generalized force vector, $M(q)$ is the inertial matrix, $N(q_1, \dot{q}_1, q_2, \dot{q}_2)$ denotes the terms of centrifugal and Coriolis's forces, the gravitational forces, elastic energy of the torsional springs at joint and the external disturbances.

The equation of motion of the proposed system can be achieved as (for detailed derivation, please see Appendix)

$$\begin{pmatrix} M + m & -\mu ml \sin \theta \operatorname{sgn}(\dot{x}) - ml \cos \theta \\ -ml \cos \theta & ml^2 \end{pmatrix} \begin{pmatrix} \ddot{x} \\ \ddot{\theta} \end{pmatrix} + \begin{pmatrix} (\sin \theta - \mu \cos \theta \operatorname{sgn}(\dot{x}))ml\dot{\theta}^2 + \mu[(M + m)g] \\ -(k\theta + c\dot{\theta}) \sin \theta / l \operatorname{sgn}(\dot{x}) \\ -mgl \sin \theta + k\theta + c\dot{\theta} \end{pmatrix} = \begin{pmatrix} 0 \\ \tau \end{pmatrix} \quad (3)$$

D. Motion generation description

In order to drive the cart to one direction by using the torque input only, the pendulum trajectory should be analyzed and planned under the coupling nature of the system. Thus two phases can be designed as follows:

- Fast motion phase: rotating the pendulum in one direction fast leads to $F_x \gg f_{max}$, thus this will drive the cart moving forward.
- Slow motion phase: rotating the pendulum in the opposite direction slowly which leads to $|F_x| < |f_{max}|$, this will keep the cart stand still.

Accordingly, the desired pendulum velocity profile shown in Fig. 2 is proposed [3]. The fast motion principle consists of phase 1 and phase 2, and the slow motion principle includes phase 3 to 6. The parametric selection is addressed in the next section.

III. SYSTEM CONSTRAINTS ANALYSIS

The aim of this research is to devise a feasible solution so that the robot can perform a thrust motion with optimality with respect to the cart displacement and the use of actuation energy. The constraints are integrated with the system dynamics to determine the feasible

solution for $\theta(t)$. In general, the constraints are as follows:

A. Constraints for the non-bounding motion phases

The cart is contact with the ground, a constraint for the contact force need to be satisfied for the whole system to achieve a non-bounding motion, in other words, the contact force has to be greater than zero, which gives

$$F_y = Mg + mg - ml\ddot{\theta} \cos \theta - ml\dot{\theta} \sin \theta - (k\theta + c\dot{\theta}) \sin \theta / l > 0, t \in [t_1, t_6] \quad (4)$$

B. Constraints for the non-sliding motion

From the duration t_4 to t_6 , the robot system remains stationary on the ground without any sliding. Thus the force of the inverted pendulum applied on the cart in the horizontal direction has to be less than the maximal static friction, gives

$$|F_x| \leq \mu F_y, t \in [t_4, t_6] \quad (5)$$

In particular,

$$\begin{aligned} & |ml\ddot{\theta} \cos \theta - ml\dot{\theta}^2 \sin \theta + (k\theta + c\dot{\theta}) \cos \theta / l| \\ & \leq \mu [Mg + mg - ml\ddot{\theta} \cos \theta - ml\dot{\theta} \sin \theta - (k\theta + c\dot{\theta}) \sin \theta / l] \end{aligned} \quad (6)$$

Furthermore, the interactive force from vertical is implicitly restricted to be non-negative under the constraint above, which essentially in virtue of the unidirectionality property of the ground.

C. Constraints for the motor

In order to avoid collisions that occur between the swinging inverted pendulum and the cart, meanwhile, the DC motor used in the proposed system is not ideal torque generator, therefore it should obey the constraint read

$$\theta_{\min} \leq \theta_t \leq \theta_{\max} \quad (7)$$

where θ_{\min} and θ_{\max} respectively represent the lower and upper boundary of the angular position of the pendulum, which are specified as follows in the proposed system

$$\theta_{\min} = -\theta_0, \theta_{\max} = \theta_0 \quad (8)$$

IV. OPTIMAL PARAMETRIC SELECTION

To maximize the displacement and average velocity of the cart, the optimum values of $t_1 \sim t_6$, P_1 , P_2 , and P_3 , which are in the desired velocity profile, need to be determined.

Using the constraints described above, the boundary conditions are defined as

$$\begin{aligned} \theta(t_2) = \theta_0, \theta(t_0) = \theta(t_6) = -\theta_0 < 0, \dot{\theta}(t_0) = 0 \\ \dot{x}(t_0) = \dot{x}(t_2) = \dot{x}(t_6) = 0 \end{aligned}$$

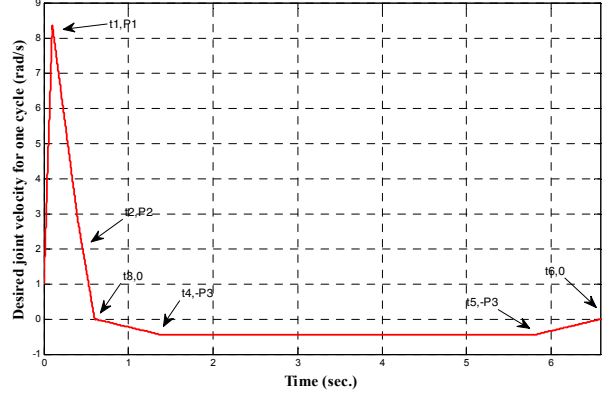


Figure 2. Desired angular velocity profile for one cycle [3]

During the fast motion phases (phase 1 and 2), i.e. $\dot{x} > 0$, the friction is negative with its maximal magnitude value. Thus integration can be conducted twice of dynamic equation (3) and take into account the initial condition. To simplify our computation, the integration related to angular position is omitted here, yields

$$(M+m)\dot{x} - ml\dot{\theta} \cos \theta - \mu ml\dot{\theta} \sin \theta + \mu(M+m)gt + C_1 = 0 \quad (9)$$

$$\begin{aligned} (M+m)x - ml \sin \theta + \mu ml \cos \theta - ml(\sin \theta_0 + \mu \cos \theta_0) \\ + \frac{1}{2} \mu(M+m)gt^2 + C_1 t + C_2 = 0 \end{aligned} \quad (10)$$

where C_1 and C_2 are constants determined by the system initial conditions.

From (9) the value of $P_2 = \dot{\theta}(t_2)$ at t_2 is

$$P_2 = \dot{\theta}(t_2) = \frac{\mu(M+m)gt_2}{ml(\cos \theta_0 + \mu \sin \theta_0)} \quad (11)$$

According to Fig.2, two area equations to satisfy the position condition for θ hold

$$\frac{1}{2} P_1 t_1 + \frac{1}{2} (P_1 + P_2)(t_2 - t_1) = 2\theta_0 \quad (12)$$

$$\frac{1}{2} [(t_6 - t_3) + (t_5 - t_4)] P_3 = 2\theta_0 + \frac{1}{2} P_2 (t_3 - t_2) \quad (13)$$

Combining (11) and (12), yields

$$P_3 = \frac{4\theta_0 + P_2(t_3 - t_2)}{t_6 - t_5 - t_4 - t_3} \quad (14)$$

$$\begin{aligned} P_2 = \left\{ \frac{\mu(M+m)g}{ml(\cos \theta_0 + \mu \sin \theta_0)} t_1 - P_1 \right. \\ \left. + \sqrt{16 \frac{\mu(M+m)g}{ml(\cos \theta_0 + \mu \sin \theta_0)} \theta_0} \right\} / 2 \end{aligned} \quad (15)$$

$$t_2 = \left\{ \frac{\mu(M+m)g}{ml(\cos\theta_0 + \mu\sin\theta_0)} t_1 - P_1 \right. \\ \left. + \sqrt{ \left(P_1 - \frac{\mu(M+m)g}{ml(\cos\theta_0 + \mu\sin\theta_0)} t_1 \right)^2 + 16 \frac{\mu(M+m)g}{ml(\cos\theta_0 + \mu\sin\theta_0)} \theta_0 } \right\} / 2 \left(\frac{\mu(M+m)g}{ml(\cos\theta_0 + \mu\sin\theta_0)} \right) \quad (16)$$

Then the desired joint acceleration and position can also be calculated through (1). Furthermore, another relationship between P_1 , P_2 , and P_0 can be found as

$$\begin{cases} P_1 = \frac{P_3(t_6 + t_5 - t_4 - t_3) - P_2(t_3 - t_1)}{t_2} \\ P_3 = \frac{P_1 t_2 + P_2(t_3 - t_1)}{(t_5 + t_6 - t_4 - t_3)} \end{cases} \quad (17)$$

Therefore, if the duration of each phase is given corresponding to the equations above, then P_1 , P_2 , and P_3 can also be determined.

V. CLOSED-LOOP CONTROLLER DESIGN

Consider the dynamic model in equation (3), the cart acceleration can be achieved as

$$\ddot{x} = \frac{1}{(M+m)} \left\{ (ml \cos\theta + \mu ml \sin\theta \operatorname{sgn}(\dot{x})) \ddot{\theta} - (\sin\theta - \mu \cos\theta \operatorname{sgn}(\dot{x})) ml \dot{\theta}^2 - \mu[(M+m)g - (k\theta + c\dot{\theta}) \sin\theta / l] \operatorname{sgn}(\dot{x}) \right\} \quad (18)$$

Spong had been studied the control of underactuated mechanical systems in his excellent papers [13], thus using the collocated partial feedback linearization technique and put (13) in (3), a feedback linearizing controller can therefore be defined as

$$\tau = \sigma(\theta)u + \xi(\theta, \dot{\theta}) \quad (19)$$

where

$$\sigma(\theta) = ml^2 - \frac{m^2 l^2 \cos\theta}{M+m} (\cos\theta + \mu \sin\theta \operatorname{sgn}(\dot{x})) \quad (20)$$

$$\xi(\theta, \dot{\theta}) = \frac{ml \cos\theta}{(M+m)} \left\{ ml(\sin\theta - \mu \cos\theta \operatorname{sgn}(\dot{x})) \dot{\theta}^2 + \mu[(M+m)g - (k\theta + c\dot{\theta}) \sin\theta / l] \operatorname{sgn}(\dot{x}) \right\} - mgl \sin\theta + k\theta + c\dot{\theta} \quad (21)$$

And if $\theta_d(t)$ represents a desired trajectory for the elastically actuated joint, then the additional control term can be defined as

$$u(t) = \ddot{\theta}_d(t) - K_v(\dot{\theta}(t) - \dot{\theta}_d(t)) - K_p(\theta(t) - \theta_d(t)) \quad (22)$$

where K_v and K_p are $m \times m$ diagonal matrix of positive gains.

Applying the control law (19) to (3) yields a linear

subsystem as

$$(\ddot{\theta}(t) - \ddot{\theta}_d(t)) + K_v(\dot{\theta}(t) - \dot{\theta}_d(t)) - K_p(\theta(t) - \theta_d(t)) = 0 \quad (23)$$

Thus appropriate values of the linear gains K_v and K_p can be selected to achieve performance requirements.

VI. SIMULATION AND COMPARISON

The parameters utilized to carry out simulation are listed in Table II. The parametric selection of elastic coefficient of the torsional spring, the coefficient of the viscous damper as well as the time nodes of the profile during one cycle are achieved through empirical approach, which will be included into our future works of inverse optimization.

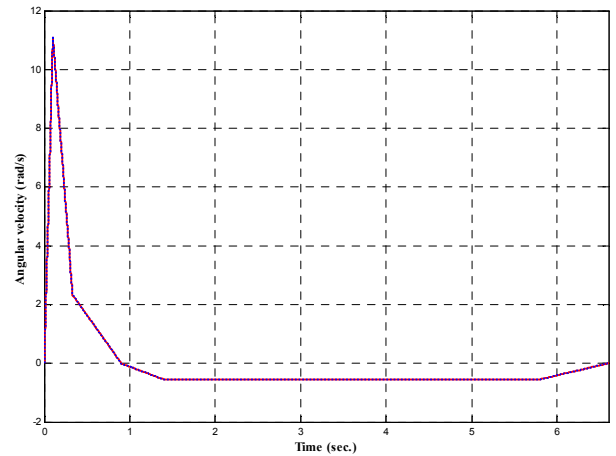
TABLE II. PARAMETRIC SELECTION

M (Kg)	m (Kg)	l (m)	μ (Nm ⁻¹ s ⁻¹)	g (m/s ²)	k (Nm rad ⁻¹)	c (Kgm ² s ⁻¹ rad ⁻¹)
=0.5	=0.05	=0.3	=0.01	=9.81	=0.15	=0.01
t ₁ (s)	t ₂ (s)	t ₃ (s)	t ₄ (s)	t ₅ (s)	t ₆ (s)	
=0.1	=0.33	=0.9	=1.4	=5.8	=6.6	

Accordingly, the desired velocity profile can be generated as

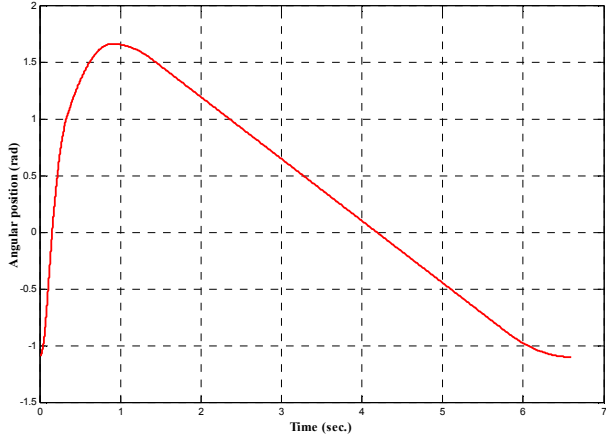
$$\dot{\theta}_d(t) = \begin{cases} 110.669t & 0 \leq t < 0.1 \\ 11.0669 - 37.97(t - 0.1) & 0.1 \leq t < 0.33 \\ -4.094(t - 0.9) & 0.33 \leq t < 0.9 \\ -0.10928(t - 0.9) & 0.9 \leq t < 1.4 \\ -0.5464 & 1.4 \leq t < 5.8 \\ 0.683(t - 6.6) & 5.8 \leq t < 6.6 \end{cases} \quad (24)$$

Fig. 3 shows the simulation results of the elastically joint-actuated cart-pole system under closed-loop control strategy for one full stroke (6.6s), in comparison with our previous system in [3]. The cart displacement showed in Fig. 3 (c) reveals that the proposed cart system moves 4.1cm within 6.6s, in contrast to 3.4cm of [3]. Moreover, it is clearly to see from Fig. 3 (a) that the desired angular velocity profile has been tracked with small errors owing to the effect of partial feedback linearization technique.

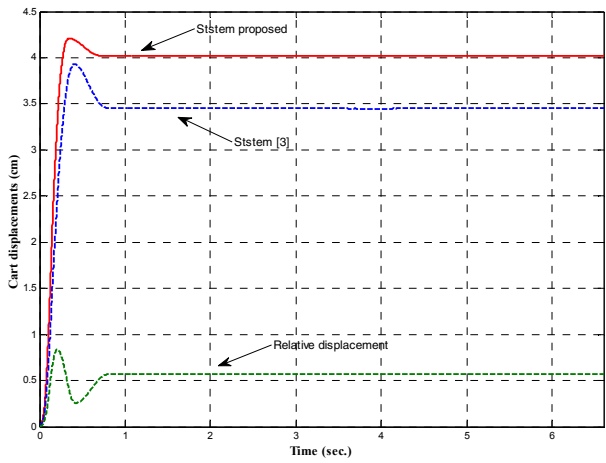


(a)

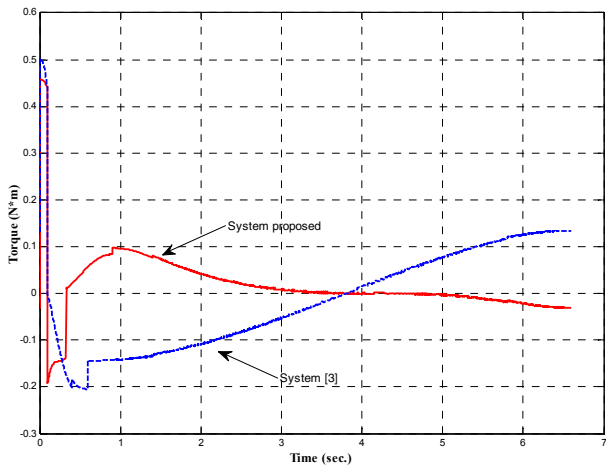
Fig. 4 and Fig. 5 demonstrate the trajectories of the cart displacement and control input for five and ten full cycles, respectively. The proposed cart system moves about 20.5cm and 40.5cm in five and ten cycles, whilst the previous system has displacements of 17cm and 34.5cm.



(b)

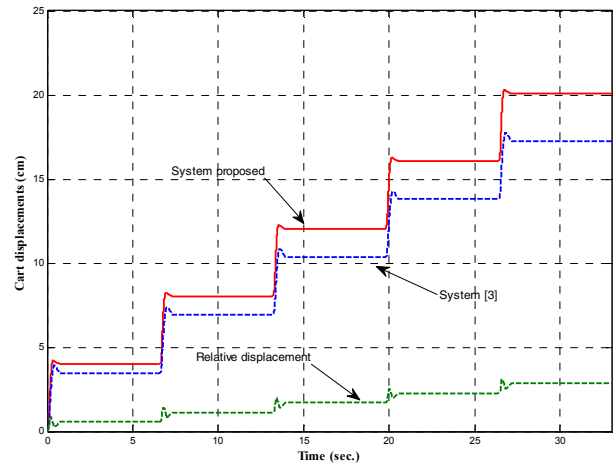


(c)

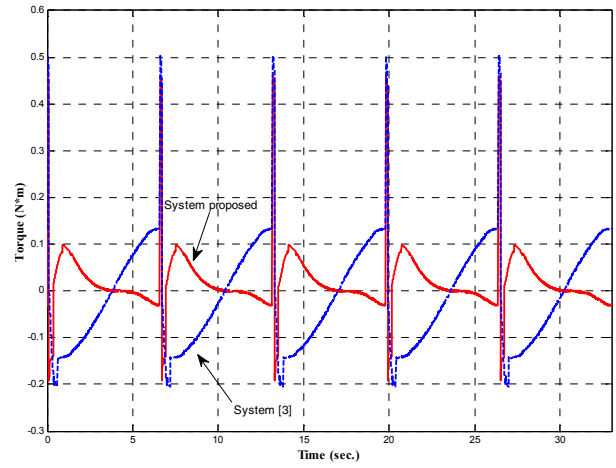


(d)

Figure 3. Trajectories under closed-loop control for one full cycle

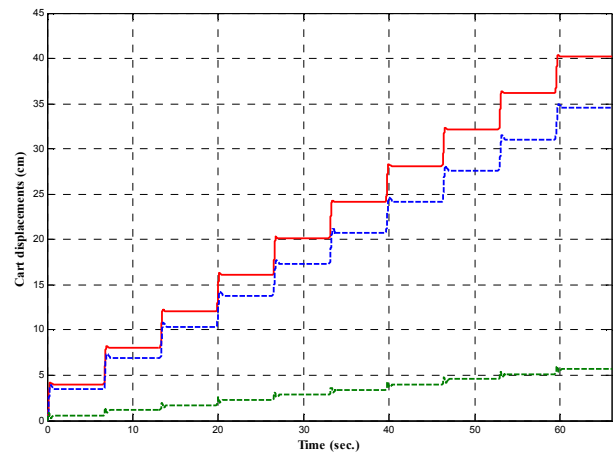


(a)

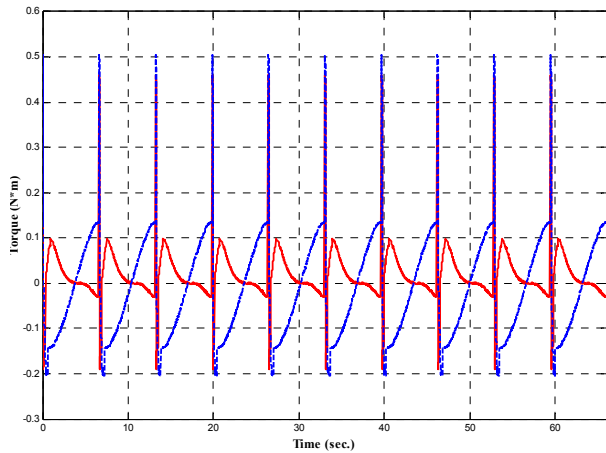


(b)

Figure 4. Comparison of trajectories of cart displacement and control input for five cycles under closed-loop control



(a)



(b)

Figure 5. Comparison of trajectories of cart displacement and control input for ten cycles under closed-loop control

The average velocity of the cart calculated from Fig. 5 for ten complete cycles is 0.53cm/s, while for the proposed elastically actuated system is 0.62cm/s. The average velocity is calculated by dividing the total travelled distance with the total required time. The proposed system travels with 16.8% higher average velocity using the proposed design, which also meant higher energy efficiency. It is more interesting to point that after twenty cycles test, the cart displacement is 81cm under the proposed system, in contrast to 68cm under system [3], which means that the cart travels almost two more cycles' displacement than [3].

VII. CONCLUSION

In this paper, a framework for the systematic modelling, optimization as well as control laws design with provable properties for the elastically joint-actuated cart-pole underactuated system is proposed, which generally shows more biological characteristics than the previous work, in particular, in storing and releasing potential energy under a predesigned trajectory, improving the rate of convergence, providing more powerful mechanical energy such that the efficacy of the robot system will be improved. The maximization approach of displacement and average velocity is adopted in this system by considering the system constraints.

The aim of this research is to investigate a novel propulsion mechanism which features more biological characteristics. It is worth mentioning that the proposed system can be used as a benchmark of elastic multibody systems like legged robots and manipulators which has extensive applications for robots in the fields of rescue, medical rehabilitation devices, haptic devices, etc. The further research which is under way focuses on the inverse optimization of the hybrid cycle (trajectory cycle mixed with spring cycle) system, and the non-integrability of the system dynamics, which are unconscious challenges to be uncovered. The research achievements will be reported in due course.

REFERENCES

- [1] Y. Liu, H. Yu, and B. Burrows, "Optimization and Control of a Pendulum-driven Cart-pole System," IEEE Int. Conf. on Networking, Sensing and Control, London, UK, April 2007.
- [2] H. Yu, T. C. Yang, Y. Liu, and S. O. Wane, "A Further Study of Control for a Pendulum Driven Cart," Int. J. Advanced Mechatronic Systems, 1(1), 2008, pp. 44-52.
- [3] H. Yu, Y. Liu, and T. C. Yang, "Closed-loop Tracking Control of a Pendulum-driven Cart-pole Underactuated System," Proc. IMechE, Part I: J. Systems and Control Engineering, 2008, 222(12), 109-125.
- [4] Y. Liu and H. Yu, "Fuzzy Control of a Pendulum-Driven Cart," Proceeding of the 2010 International Conference on Modelling, Identification and Control, pp. 698-703, 2010.
- [5] Y. Liu, H. Yu, and T. C. Yang, "On Tracking Control of a Pendulum-driven Cart-pole Underactuated System," International Journal of Modeling, Identification and Control, Vol. 4, No. 4, pp. 357-372, 2008.
- [6] Y. Liu, H. Yu, L. Vladareanu, S. Cang and F. Gao, "trajectory panning of a pendulum-driven underactuated cart," MEC-APPL, 2011.
- [7] R. McN. Alexander, N. J. Dimery, and R. F. Ker, "Elastic structures in the back and their role in galloping in some mammals," J. Zoology (London), vol. 207, pp. 467-482, 1985.
- [8] Gill A. Pratt, and Matthew M. Williamson, "Series Elastic Actuators," IEEE International Conference on Intelligent Robots and Systems, vol. 1, pp. 399-406, 1995.
- [9] Matthew M. Williamson, "Series Elastic Actuators," M.S. thesis, Massachusetts Institute of Technology, June 1995.
- [10] D.W. Robinson, J.E. Pratt, D.J. Paluska, and G.A. Pratt, "Series Elastic Actuator Development for a Biomimetic Walking Robot," IEEE/ASME International Conference on Advanced Intelligent Mechatronics, Sept. 1999.
- [11] David W. Robinson, "Design and Analysis of Series Elasticity in Closed-loop Actuator Force Control," PhD. thesis, Massachusetts Institute of Technology, June 2000.
- [12] R. McN. Alexander, "Three Uses for Springs in Legged Locomotion," The International Journal of Robotics Research, vol. 9, pp. 53-61, 1990.
- [13] M. Spong, "Underactuated Mechanical Systems," Control Problems in Robotics and Automation, Lecture Notes in Control and Information Sciences, vol. 230, pp. 135-150, 1998.
- [14] R. McN. Alexander, G. M. O. Maloij, R. F. Ker, A. S. Jayes, and C. N. Warui, "The role of tendon elasticity in the locomotion of the camel," J. Zoology (London), vol. 198, pp. 293-313, 1982.
- [15] G. A. Cavagna, H. Thys, and A. Zamboni, "The source of external work in level walking and running," J. Physiol., vol. 262, pp. 639-657, 1976.
- [16] T. A. McMahon, "The role of compliance in mammalian running gaits," J. Exp. Biol., vol. 115, pp. 263-282, 1985.
- [17] G.A. Pratt, "Low Impedance Walking Robots," Integrative and Comparative Biology, vol. 42, pp. 174-181, 2002.
- [18] G. A. Pratt and M. M. Williamson, "Series elastic actuators," in International Conference on Intelligent Robots and Systems, 1995.
- [19] N. J. Dimery, R. McN. Alexander, and R. F. Ker, "Elastic extension of leg tendons in the locomotion of horses," J. Zoology (London), vol. 210, pp. 415-425, 1986.
- [20] J.E. Pratt, B.T. Krupp, "Series Elastic Actuators for legged robots," Proceedings of SPIE - the international society for optical engineering, 2004.